Designing polymer nanocomposites with a semi-interpenetrating or interpenetrating network structure

Controlling the mechanical behavior of polymer nanocomposites by incorporating nanoparticle network

Wenhui Wang[1], Guanyi Hou[1], Yishuo Guo[1], Lu Wang[1], Jun Liu[1,2,3,4*], Youping Wu[1,2,3], Liqun Zhang[1,2,3,4,5*], Alexey V. Lyulin[6*]

*Corresponding author: liujun@mail.buct.edu.cn or zhanglq@mail.buct.edu.cn or a.v.lyulin@tue.nl

[1]Key Laboratory of Beijing City on Preparation and Processing of Novel Polymer Materials, Beijing University of Chemical Technology, People's Republic of China

[2]Beijing Engineering Research Center of Advanced Elastomers, Beijing University of Chemical Technology, People's Republic of China

[3]Engineering Research Center of Elastomer Materials on Energy Conservation and Resources, Beijing University of Chemical Technology, People's Republic of China

[4]Beijing Advanced Innovation Center for Soft Matter Science and Engineering, Beijing University of Chemical Technology, 100029 Beijing, People's Republic of China

[5]State Key Laboratory of Organic-Inorganic Composites, Beijing University of Chemical Technology, 100029 Beijing, People's Republic of China

[6]Group Theory of Polymers and Soft Matter, Department of Applied Physics, Technische Universiteit Eindhoven,5600 MB, Eindhoven, The Netherlands

Abstract

Using short polymer chains, through molecular dynamics simulation we design a well-dispersed nanoparticle (NP) network which is then incorporated into the polymer matrix. We examine the effects of the end-grafted chain flexibility and density on the dispersion of the NPs, the dimension of the polymer matrix chains and the penetration depth of the polymer matrix into the NP network. Furthermore, by changing the interactions strength between the matrix polymer chains and the end-grafted ones while fixing the number of the grafted chains and its flexibility in the single-network system(NP network), we analyze the interfacial state between polymer matrix and NP network by calculating the total interaction energy between the polymer matrix chains and the grafted chains. Meantime, the uniaxial tensile stress-strain behavior and the orientation extent of the matrix and grafted polymer chains along the uniaxial tensile deformation direction influenced by the interaction strength between the matrix polymer and the grafted chains are investigated, both for the single-network system

and the double-network system (NP network and matrix network). In particular, for the double-network system, we modulate the integrity of the NP network ranging from 0% to 100%, which corresponds to the gradual transition of the dispersion morphology of the NPs from the aggregation state to the uniform dispersion state, and tensile deformation similar to the single network system is performed. Accompanying this, the mechanical reinforcing efficiency increases gradually, which is attributed to the much greater orientation of grafted and matrix polymer chains induced by the enhanced dispersion of the NPs. By simulating the storage modulus as a function of the strain amplitude in the single-network system, the non-linear behavior (the famous Payne effect) is seen to decrease with the increase of the NP network integrity because of the improved dispersion of the NPs. In general, our results could provide a new approach to design of high performance polymer nanocomposites by taking advantage of the nanoparticle network reinforcing unit.

1.Introduction

The development of tires with optimized structure and high performance has always been a significant issue both academically and industrially, for the fact that the performance of automobiles such as their environmental affinity, traction and mileage relies largely on the tires' material components including the microscopic structure and the macroscopic mechanical properties. Importantly, tires with excellent tensile and tear strength, together with low energy dissipation are ideal candidates to meet the practical service. Consequently, the mechanical reinforcement of rubber matrix has been a critical topic. Tang et al.[1] demonstrated recently a bio-inspired design of high performance and macroscopically responsive diene-rubber by engineering sacrificial metal−ligand motifs into a chemically crosslinked architecture network, which improves the modulus, tensile strength, and toughness of the systems while lessens dissipated energy at the same time. Through small-angle neutron scattering (SANS), Gold et al.[2] examined the enhanced mechanical properties of the dual polybutadiene networks and found a homogeneous distribution of the transient bonds in both the

functionalized polymers and the dual network products acting as sacrificial bonds that dissipate energy. Similar sacrificial networks have been exploited by Creton et al.[3], Guo et al.[4] and Huang et al.[5] to enhance the mechanical properties of the rubber matrix and reduce energy dissipation. Moreover, Liu et al.[6] established a carbon nano-spring structure, which proved to be very effective to lower the hysteresis loss, resulting in the reduction of the energy dissipation of the elastomeric polymer materials.

Besides designing and facilitating the sacrificial bonds and carbon nano-spring structure, incorporating nanoparticles (NPs) into polymer matrices has proven to be an effective approach to regulate the mechanical and viscoelastic properties of polymer nanocomposites (PNCs).[7, 8, 9, 10] Balazs et al.[11] pointed out that the mixing of polymers and nanoparticles generates composites materials with advantageous electrical, optical, or mechanical properties with potential hierarchical structure. It has been commonly acknowledged that a uniform dispersion of nanofillers in the polymer matrices is a general prerequisite for achieving desired mechanical and physical characteristics.[12] One effective way is to uniformly graft the NPs with short polymer chains.[13, 14, 15, 16] Actually, the incorporation of the grafted NPs into the polymer matrix contributes a lot in modulating the spatial dispersion of the NPs in the polymer matrices, which is promoted by the development of the synthesis techniques to controllably functionalize NPs with polymer chains.[17, 18] Through the rheology analysis of polymer-grafted NPs filled polymer nanocomposites, Moll et al [13]concluded that the formation of a transient, long-lived, percolating polymer-NPs network with the NPs serving as the network junctions contributes to the maximum mechanical reinforcement. Notably, Akcora et al.[19] found that the grafted spherical NPs can robustly self-assemble into a variety of anisotropic superstructures when dispersed in the corresponding

homopolymer matrix, enabling considerable control for the fabrication of polymer nanocomposites with enhanced mechanical properties. Besides a lot of experimental trials, much computational simulation work at the microscopic level carried out by Chao et al.[20], Yan et al.[21]and Liu et al. have also perceptually and theoretically verified that the incorporation of the grafted-NPs, either spherical NPs[22, 23]or anisotropic ones[24, 25], into the polymer matrix can well enhance the mechanical properties of the polymer nanocomposites, guiding a promising precise design for various structure of polymer nanocomposites. As a matter of fact, in the conventional polymer nanocomposites, the energy loss of the polymeric nanocomposites materials stems mainly from the dynamic fillers-fillers, fillers-polymer chains and polymer chains-polymer chains contacts, as well as the high mobility of polymer chain ends. Therefore, facilitating the dispersion of the fillers and decreasing the mobility of the free ends of the polymer chains are vital and effective approaches to balance the mechanical reinforcement and the energy dissipation.

Very recently, Creton etal.[26] created a first network by polymerization of monomers, and then swelled it with corresponding monomers, such as EA(ethyl acrylate), MA(methyl acrylate) and BA(butyl acrylate), which were further polymerized to form the soft extensible matrix network. They found that the stiffening at high strain in these multiple networks can well be tuned. Baeza et al.[27] regulated the character of polymer bridges which physically tie NPs together into a network and performed the rheological measurements on favourably interacting mixtures of spherical silica NPs and poly(2-vinylpyridine). In their study, the system dynamics are polymer-like with increased friction for low silica loadings, and it gradually turns into the network-like when the mean face-to-face separation between NPs becomes smaller than the entanglement tube diameter. The results reveal that the flow

properties as well as the mechanical properties of the nanocomposites systems can be tuned via establishing a kind of virtual NP network formed by adsorption interactions between the NPs and the polymers.

In experiment, Seo et al.[28] first proposed a concept for reinforcing silica, named networked silica, which was used to achieve enhanced reinforcing performance of silica and to eliminate the disadvantage of ethanol production and precure through coupling reagents in the preparation of silica-reinforced SBR compounds. The networked silica was prepared by connecting silica particles with amine and glycidoxy groups, which was then compounded in SBR, exhibiting a significant enhancement of the tensile strength accompanied with a moderate increase of the modulus at a high loading of 70 phr even without using any coupling reagents. In another study[29], they prepared a networked silica using bis-(triethoxysilylpropyl)-tetrasulfide (TESPT) as a connecting chemical at various loading levels. They found that the styrene–butadiene rubber (SBR) compounds reinforced with the networked silica exhibited low filler–filler interaction and high rubber–filler interactions due to the entanglements between the rubber molecules and the connecting chains of the networked silica. Meantime, the increased physical interactions improved the elastic properties and the wear resistance, while lowering the rolling resistance of the rubber compounds, resulting in long tire service life and high automobile fuel efficiency. The enhanced physical properties of the SBR compounds reinforced with the networked silica support their promising potential as reinforcing fillers for tire manufacture.

Based on the networked silica system, it is noted that although several experimental studies have been carried out to investigate the networked silica system, little was known about how to regulate the structure thus to optimize its mechanical

properties. More fundamental understanding of the structure of the networked NPs connected by short chains and its resulting mechanical properties are to be acquired. In this work, by taking advantage of molecular dynamics simulation, we successfully design a networked NPs in which the NPs are chemically bonded with dual-end functionalized short chains, which is then incorporated with the polymer matrix. We then investigate how to control the dispersion of NP network and the penetration of the polymer matrix by particularly varying the number and the flexibility of the grafted chains, as well as the interfacial interaction between the polymer matrix and the NP network. Most significantly, the resulting mechanical properties of the materials are simulated, aiming to provide a scientific guidance for the design and fabrication of PNCs with remarkable and adjustable mechanical properties in practical applications.

2. Simulation model and method

In the present study, a coarse-grained model of the nanoparticle-network linked via short chains embedded in chemically identical polymer matrix was adopted. The polymer chains are represented by the classical bead-spring model together with a bending potential, in which each bead corresponds to 3-6 bonds of a realistic polymer chain. There are four types of Lennard-Jones (LJ) beads in the simulation box initially (see Table 1), before the nanoparticle network is formed. The diameter of a NP is four times that of a polymer bead. According to the mapping process[30, 31], the modeled NP with the diameter equal to 10σ generally maps to the 12.8 nm or 28.8 nm-diameter silica particles. Thus, the NP with the diameter equal to 4σ in the present simulation model corresponds to approximately 5–12 nm silica particles when mapping the coarse-grained model to real NPs. There are 20 NPs chemically linked with a certain

number of short chains, varied from 200 to 300, to form a thermally stable nanoparticle network. Herein each short grafted chain consists of 45 beads and is dual-end linked to NPs to achieve a distinct network structure, as shown in Figure 1(a). The matrix polymer chain shown in Figure 1(b) is composed of 100 beads. It is noteworthy that although these polymeric chains are short, they have already shown the static and dynamic behavior characteristics of the polymer chains. The non-bonded polymer-polymer, polymer-nanoparticle, nanoparticle-nanoparticle interactions are modeled by the expanded truncated and shifted Lennard-Jones (LJ) potential

$$U=\begin{cases} 4\varepsilon\left[\left(\dfrac{\sigma}{r-\Delta}\right)^{12}-\left(\dfrac{\sigma}{r-\Delta}\right)^{6}\right]+C & r<r_{cutoff}+\Delta \\ 0 & r\geq r_{cutoff}+\Delta \end{cases} \quad (1)$$

where ε is the pair interactions energy parameter, r is the distance between two interaction sites, and Δ takes into account the effect of the excluded volume of different interaction sites. Hence, the actual cutoff distance is the sum of r_{cutoff} and Δ. For the polymer-polymer, polymer-nanoparticle and the nanoparticle-nanoparticle interactions, the values of Δ are equal to zero, $R_{NP}-\sigma/2$ and $2R_{NP}-\sigma$, respectively. The LJ potential is cut offat different distances to model the attractive or repulsive interactions. The r_{cutoff} stands for the distance at which the interactionsare truncated and shifted so that the energy is equal to zero at this distance. The polymer-nanoparticle interactions parameters are set as $r_{cutoff}=2.5\sigma$ originally to form NP network, which are then modified to be $r_{cutoff}=2^{1/6}\sigma$ to simulate the realistic systems. The polymer-polymer and the nanoparticle-nanoparticle interaction

parameters are both set as $r_{cutoff} = 2.5\sigma$ in the simulation systems. C in Eq. (1) is a constant guaranteeing the condition U=0 when $r = r_{cutoff} + \Delta$. In the present simulations, the nanoparticle-nanoparticle interactions energy parameter ε_{nn} is firstly set to be 100.0 to form a network structure, and is further changed to 1.0 to simulate the interaction strength between nanoparticles. The corresponding nanoparticle-polymer interactions energy parameter ε_{np} and polymer-polymer interactions energy parameter ε_{pp} are both set to be 1.0. Since we are not aiming at studying a specific polymer, the mass m, the diameter σ of each bead, and the interactions strength ε are all set equal to unity, and all calculated quantities are dimensionless.

The interaction between the adjacent bonded beads is modeled by a harmonic potential:

$$U_{bond} = \frac{1}{2} K (r - r_0)^2 \qquad (2)$$

where K is the bond strength and r_0 is the equilibrium bond distance. If the bond is created between polymer beads, K and r_0 are equal to $1000.0\,\varepsilon/\sigma^2$ and $1.0\,\sigma$, respectively. These constants are set to be $2000.0\,\varepsilon/\sigma^2$ and $2.5\,\sigma$, respectively, if the bond is created by a NP and a grafted polymer bead. The K and r_0 values are chosen to ensure a certain stiffness of the bonds while avoiding the high-frequency modes and chain crossing. Herein r is the separation distance between two connected interaction sites.

The bending angle of polymer chain between three consecutive beads is modeled by a cosine potential:

$$E_{angle}(\theta) = k(1 + \cos\theta) \qquad (3)$$

where k is the bending energy, θ is the angle between three consecutive beads. In this work, k is equal to 0 for matrix polymeric chains, denoting the matrix polymer to be flexible. The value of k for the grafted chains varies from 0 to 1000 to change the flexibility of grafted chains. For better comparison, all the force-field parameters are listed in Table 2.

The *NPT* and *NVT* ensembles are both adopted in the present MD simulations, where the temperature is mostly fixed at $T^* = 1.0$, and the pressure is set to be $P^* = 1.0$ by using the Nose-Hoover thermostat and barostat. The velocity-Verlet algorithm is used to integrate the equations of motion with a time step $\delta t = 0.001$, where the time is reduced by $\tau = \sigma\sqrt{\frac{m}{\varepsilon}}$. The periodic boundary conditions are used in all three directions.

Before the nanoparticle network is formed, the original system including NPs, dual-end functionalized short polymer chains and polymer matrix chains has been equilibrated under the *NPT* ensemble over a long time so that each chain has moved at least $2R_g$, where R_g is the root mean square radius of gyration of polymer matrix chains. After this, a *NPT* ensemble is adopted and the dual-ends functionalized short polymer chains are grafted onto the surface of the NPs. Once a dual-end functionalized short polymer chain-end approaches any NP, a chemical bond is formed between these two interaction beads. Note that this new chemical bonding is modeled by the same harmonic potential as other bonded potentials. Both ends of a short chain are grafted onto NPs and one functionalized end can only be bonded with one NP, while one NP can be bonded with a certain number (20, 25 or 30) of functionalized ends. Therefore, a loop structure or bridge structure, shown in Figure1(a)can be formed in the assembly of one short grafted chain with two

NPs.Atthe end of these rather time-consuming simulations, all the NPs and the dual-end functionalized short polymer chains are made into one network through chemical bonding. This network is further embedded in the matrix polymers (see below). The NVT ensemble is then adopted to further equilibrate the systems, where the temperature is kept at $T^* = 1.0$, and the volume of the simulation box is fixed throughout the whole simulation process.

In this simulation work, initially the polymer matrix is not crosslinked, denoting only one network formed by NPs and short grafted chainsis present in the total system. We define this as the single-network system. In the present study we also crosslink the polymer matrix for further discussions(see the discussions later in "Tensile mechanical properties" part).By randomly selecting pairs of polymer beads within a distance of 1.5σ from each other, and tethering them together by means of the harmonic potential, permanent crosslinked bonds are imposed in the matrix polymeric chains to form another matrix polymeric network. The resulting structure, containing the NP network as well as the matrix polymeric network, is called double-network system.

In the present simulations, the following approach to perform the tensile deformation has been used, following our previous studies.[32] The box length in the Z direction is increased at a constant engineering strain rate, while the box lengths in the X and Y directions are reduced simultaneously so as to maintain a constant box volume. The interactions between atoms in the basic cell and image atoms across the cell wall serve to transmit the deformation to the atoms in the basic cell. The strain rate is specified as $\dot{\varepsilon} = \left(L(t)_Z - L_Z\right) / L_Z / \tau = 0.0327 / \tau$. The average stress σ in the Z direction is obtained from the deviatoric part of the stress tensor $\sigma = (1+\mu)(-P_{ZZ} + P) \approx 3(-P_{ZZ} + P)/2$, where $P = \Sigma_i P_{ii} / 3$ is the hydrostatic

pressure. The parameter μ stands for the Poisson's ratio, which is equal to 0.5 in our simulations.

For the oscillatory shear deformation, we use the SLLOD equations of motion[33] and the Lees-Edwards "sliding brick" boundary conditions[34] are adopted. The upper XY plane of the simulation box is shifted along the X direction so that each point in the simulation box can be considered as having a "streaming" velocity. This position-dependent streaming velocity is subtracted from the actual velocity of each atom to yield a thermal velocity, which can be used for temperature computation and thermostatting. The shear strain is defined as $\gamma = \delta_X / L_Z(0)$, where the offset δ_X is the transverse displacement distance in the shear direction (X direction for XY deformation) from the unstrained orientation, and $L_Z(0)$ is the box length perpendicular to the shear direction. We set the shear strain rate $\nu = 0.01/\tau$, i.e., imposing one cycle of constant-amplitude oscillation every 100τ. The average shear stress is obtained from the deviatoric part of the stress tensor $\delta_S = P_{XY} = P_{YX}$.

All MD runs are carried out using the large scale atomic/molecular massively parallel simulator (LAMMPS) software developed by Sandia National Laboratories.[35] More simulation details can be found in our previous publications.[36, 37, 38]

3. Results and discussion

3.1 Structure tuned by the grafted chain density and flexibility

To obtain a fine NP network structure by linking NPs via short polymer chains, the following procedure is adopted. Starting from a uniform blends including NPs, dual-end functionalized short chains and matrix polymeric chains, we set strong interactions between the functionalized ends of the short polymer chain and NPs,

therefore a chemical bonding is produced when the distance between the functionalized ends and the NPs is small enough. Through this approach, we manage to graft functionalized-ends of all short chains onto NPs and successfully establish a three-dimensional chemical network by using NPs as net points, as shown in Figure 1. It can be theoretically inferred that the NPs are homogeneously dispersed in the polymer matrix. In order to accurately regulate the structure, we take account of the effects of the grafting chain density and chain flexibility on the dispersion of the three-dimensional network structure.

3.1.1 NPs dispersion

In Figure 2 we show the mean-squared end-to-end distance R_{eed}^2 of polymer matrix chains as a function of the simulation time in single network systems with varying flexibility and density of grafted chains, aiming to ensure that well-equilibrated systems are obtained. We can easily see in Figure 2(a) that more rigidity of grafted chains leads to larger size of matrix chains, and in Figure 2(b) that more density of grafted chains results in larger size of matrix chains, too. However, the most important information shown in Figure 2 is that the systems have been properly and fully equilibrated when the variable R_{eed}^2 (matrix) of the systems tend to be steady. Following this, we examine the effect of the grafted chain flexibility on the dispersion of NPs. The radial distribution function between NPs is used to characterize the dispersion of NPs, as is shown in Figure 3(a), (b) and (c). We fix the number of grafted chains at $N_g = 200$, thus the only variable is the grafted chain

flexibility. The flexibility of grafted chains is regulated by the bending energy, namely the value of k in Eq.(3). Larger bending energies represent more rigid grafted chains, such as $k = 0$, $k = 500$ and $k = 1000$ denote flexible, slightly rigid and strong rigid grafted chains, respectively. For better comparison as well as to present the figures more clearly, we omitted the previous part (with $g(r)_{nn}$ equals zero) of the figures until any peaks appear. Apparently, for the systems with these three different rigidities, the first peaks appear approximately at the distance 6.5σ, 6.7σ and 7.5σ, respectively, and no peaks occur at around 4σ, indicating no direct contact state of NPs (with diameter equals 4σ). The position of the occurrence of the first peak implies that the NP network becomes much larger by increasing the rigidity of the grafted chains. When it comes to the effect of the grafted chain density(denoted by N_g) on the dispersion of the NPs, we change the number of the grafted chains from 200 to 300, while the grafted chains are all set to be slightly rigid($k = 500$). The radial distribution functions of NPs shown in Figure 3(d), (e) and (f)indicate that a better dispersion of the NPs is obtained with an increasing number of the grafted chains, which can be explained in the same way as in that of Figure 3(a), (b) and (c). Herein the position of the appearance of the first peak shows less difference from each other, but this particular slight variation tendency still verifies that denser grafted chains leads to larger size of NP network. To further testify the dispersion of NPs, we quantitatively calculate the average number of NPs within a certain distance away from each other in the simulation box. Figure 3(g) shows the results obtained by counting the number of NPs within a distance $r < 12.0$ from each other, by focusing on

the effects of the grafting chain density and chain flexibility. The grafted polymer chains get more rigid as the value of k increases. It is clearly evidenced that the columnar bars gradually become lower with the increase of the rigidity of the grafted chains by fixing the grafting density. The lower columnar bars mean less NPs aggregation, or better NPs dispersion morphology. The same conclusion applies to the case when merely increasing the number of the grafted chains while the flexibility of the grafted chains is set. The results suggest that increasing the rigidity and density of the grafted chains on NPs can both contribute to the dispersion of the NPs, resulting in a larger and more distinct NP network. It can be explained as follows: as the grafted chains are dual-end linked to NPs, all NPs are restrained by the short grafted chains, thus the mobility of NPs is bound to the network. As the rigidity of the grafted chains increases, the functionalized ends of the grafted chains begin to stretch, which promotes longer distance between the dual-end linked NPs. In the same way, by increasing the number of the grafted chains, each NP is linked by more grafted chains, which significantly prevents NPs from approaching each other, therefore a well dispersed morphology is achieved.

3.1.2 Penetration of polymer matrix into the nanoparticle network

Apart from the NPs dispersion , the penetration of matrix polymer chains into the NPs network is the other vital physical parameter of the network structure. As is shown in Figure 4(a), we calculate the total interaction energy U_{gm} between matrix chains and short grafted chains as a function of the grafted chain flexibility as well as the number of the grafted chains to reflect the incorporation state of matrix polymers

into the NPs network. Note that the matrix polymer chains and the short grafted chains are chemically identical. It is clearly shown that when fixing the number of grafted chains at $N_g = 200$, the total interaction energy between the matrix polymer chains and the short grafted chains increases gradually with the gradual transition of the rigidity of the grafted chains from the flexible state to the rigid state. Meanwhile, fixing the number of the grafted chains at $N_g = 250$ or $N_g = 300$, the total interaction energy between the matrix polymer chains and the short grafted chains increases slowly at first, but drops off latterly. After reaching a peak at $k = 500$, the total interaction energy between the matrix polymer chains and the short grafted chains begins to decrease by a further increase of the rigidity of the grafted chains. This is due to the fact that the number of the grafted polymer chains equal to 200 is relatively sparse compared with 250 or 300 of grafted chains when the total number of NPs is fixed. As described above, since the NPs are interconnected by the grafted chains to form a network structure, improving the chain rigidity will surely lead to the expansion of the NPs network, which consequently promotes the penetration of the flexible matrix polymer chains into the NPs network. However, this explanation only applies to the case when the grafted chain density is low. When it comes to the case where $N_g = 250$ or $N_g = 300$, the situation becomes a little different although the dispersion of NPs and the general total interaction energy between the matrix polymer chains and the short grafted chains are truly better than that of $N_g = 200$. A better dispersion of NPs does not necessarily mean that the matrix polymers will surely penetrate into the NPs network more easily. In actual, it is more difficult for the

matrix polymers to penetrate into the NPs network when the network is rather dense as well as rigid enough, that is to say, too much rigidity of the dense network will make it difficult for the polymer matrix to penetrate. That explains a stronger total interaction energy between the matrix polymer chains and the short grafted chains at $N_g = 250$ than that of $N_g = 300$. To further clarify the effect of the rigidity of the grafted chains on the penetration of matrix polymers into the NPs network, we calculate the radial distribution function between NPs and the matrix polymer chains beads by fixing $N_g = 250$, shown in Figure 4(b). The results show that the increase of the rigidity indeed contributes to the dispersion of NPs, as is explained by the higher content of matrix polymers in the vicinity of NPs within approximately 4σ when k is equal to 1000, corresponding to a rigid grafted chains. However, when k is equal to 500, it can be seen that within the distance ranging from 4σ to 12σ, corresponding to the network structure region, the content of matrix polymers is significantly higher than that for k=0 or k=1000, which signifies a better incorporation of matrix polymers within the network structure. At last, it is noteworthy that when the number of the grafted chains is equal to 250 and the value of the rigidity parameter k is 500, a relatively fine NPs dispersion with a good matrix penetration state is observed. Thus an integrated structure of NPs network immersed in the polymeric matrix is basically obtained.

3.2 Tensile mechanical properties

By taking advantage of the optimal dispersion state, we also investigate the effect

of the interfacial interaction strength ε between matrix polymers and grafted chains on the interfacial structure, by calculating the total interaction energy U_{gm} between the matrix polymer chains and the grafted chains. As is shown in Figure 5(a), the total interaction energy between the matrix polymer chains and the grafted chains increases obviously with the gradual augment of the interfacial interaction strength ε, with the lowest interfacial energy appearing when the interaction becomes purely repulsive between matrix polymers and grafted chains. This result indicates that stronger interfacial interaction strength contributes to better incorporation of matrix polymers into the NP network.

Based on previous analysis, the incorporated NPs network forms a uniform dispersion state in the polymer matrix. Theoretically, this network incorporation structure should exhibit an excellent mechanical reinforcement, attributed to the good dispersion of NPs and the interfacial interaction between polymer and NPs network. Therefore, we further examine the tensile stress-strain behavior of this structure of NP network immersed in the polymer matrix. Here we explore the effect of the interfacial interaction strength ε between matrix polymers and grafted chains on the tensile stress-strain behavior as well as the orientation behavior of the system during the uniaxial tensile deformation process. Figure 5(b) shows that the tensile stress monotonically increases with the tensile strain, and apparently stronger interfacial interaction strength ε between matrix polymers and grafted chains leads to much greater stress strength, implying a better mechanical reinforcement.

Furthermore , to probe the orientation of the matrix polymer chains and the grafted chains during the tensile deformation process, we use the second-order Legendre polynomials $< P_2(cos\theta) >$

$$\left\langle P_2\left(\cos\theta\right)\right\rangle = \left(3\left\langle \cos^2\theta\right\rangle - 1\right)/2 \qquad (4)$$

to characterize the bond orientation, where θ denotes the angle between a given element (two adjoining monomers in the chain) and the reference direction (the stretching direction). The possible values of $< P_2(cos\theta) >$ range from -0.5 to 1, and the value of -0.5, 1 and 0 indicate a perfect orientation perpendicular to the reference direction, parallel to the reference direction or randomly oriented, respectively. Obviously, as seen from Figure 5(c),both grafted chains and matrix (not shown here) polymer chains orientate more distinctly along the deformation direction during the tensile process, but neither of them is strongly dependent on the interfacial interaction strength ε between matrix polymers and grafted chains. However, when we keep the interfacial interaction strength ε between matrix polymers and grafted chains constant, it is notable in Figure 5(d) and 5(e) that the orientation of the grafted chains is much better than that of the matrix polymer chains. The underlying reason is that the grafted chains are drawn by NPs to orientate along the stretching direction, while the matrix chains are relatively free to move randomly compared to the former. To further investigate the tensile behavior of the system as well as to provide more valuable guidance for industrial products such as vulcanized rubber nanocomposites, we create a double-network system (as we have introduce before), which is produced by crosslinking the matrix polymer chains incorporated with the original NP network.

We obtain crosslinked matrix polymers with precisely 600 crosslinked bonds in the present simulations. After the double-network system reaches its thermodynamic equilibrium state, similar tensile deformation process is exerted on the system. We focus on the tensile stress-strain behavior and the chain orientation of the double-network system, Figure 6 shows analogical results as that of the single-network system in Figure 5. Stronger interfacial interaction between matrix polymers and grafted chains contributes to much better mechanical behavior of the double-network system during the stretching process. The grafted chains are oriented much more strikingly along the stretching direction than that of the matrix polymer chains, because of the pulling effect of the NPs. Besides, the extension of the crosslinked polymer matrix chains can be inhibited by the crosslinking effect to some extent. We can see that the attractive interfacial interaction between matrix polymers and grafted chains promotes the orientation of the matrix polymer chains along the tensile direction, while the repulsive interaction contributes less, which implies that the orientation of chains is vitally affected by the pulling effect of NPs. To demonstrate the effect of NP network integrity on the mechanical property of the double-network system, uniaxial tensile deformation is exerted on the double-network systems with various integrity degree of NP network. The network integrity here is referred to the ratio of the number of the crosslinked bonds of the partial NP network (initially perfect NP network being broken artificially) to that of a perfect NP network. A larger NP network integrity signifies a less-broken NP network. The NP network integrity ranges from 0% to 100%, corresponding to the transition of the dispersion

morphology of the NPs from the aggregation state to the uniform dispersion state.The stress-strain curve in Figure 7(a) shows that larger stress strength is obtained when the NP network is less broken in the double-network system. As is shown in Figure 7(b), the breakage of the NPs network leads to less orientation of the grafted chains, caused by the reduction of NPs pulling effect, while the effect of the breakage of the NPs network on the orientation of the matrix polymer chains (not shown here)is relatively weaker compared to the former, which supports the previous conclusion that the orientation of chains is significantly affected by the pulling effect of NPs.

3.3 Dynamic shear mechanical properties

Furthermore, we investigate the effect of the NP network integrity on the non-linear behavior of the flexible single-network systems. We mainly focus on the Payne effect of the systems, namely the amplitude-dependence of the storage modulus. To ensure the reliability and stability of the data used for the curve fitting, we collect the simulated stress data in the latter 10 deformation cycles of all 15 cycles and the storage modulus as a function of the dynamic strain amplitude for simulated systems is obtained.

By varying the degree of the integrity of NPs network, the variation of the storage modulus shown in Figure 8 as a function of the strain amplitude suggests the change of the total nanoparticles interaction energy of the systems. Notably, the storage modulus of the non-NP-network composites is the highest among all these systems atlow strain amplitude, and decreases quickly with the increase of the shear strain amplitude, reflecting a strong Payne or non-linear effect. The decrease of the storage modulus of the compounds at the high strain is presumably caused by the breakdown

of the NPs-NPs interactions. We can come into the conclusion that a poor dispersion or strong agglomeration of the NPs results in much higher NPs-NPs interactions and higher storage modulus at a low strain, while the increase of the strain leads to strong destruction of the NPs-NPs interaction, resulting in the rapid decrease of the storage modulus, which can be supported by the experimental work of Seo etal.[29] Meantime, compared to that of the non-NP-network composites system, in the polymer composites system containing 40% NP-network structure, the existence of a certain extent of NP network reduces the possibility of direct strong interactions among the NPs, thereby lowering the storage modulus at small strain amplitude. However, on the other hand, due to the damage of 60% NP-network structure, there is still a certain content of agglomeration of the NPs, which leads to relatively high NPs-NPs interactions and higher storage modulus at a low strain compared to the full-NP-network composites. By increasing the stain amplitude, the storage modulus of this system shows similar behavior as the non-NP-network composites system, with a slightly smaller decreasing tendency caused by the existence of NP-network structure part. A similar result is obtained in the 80% NP-network polymer composites system, which indicates much less reduction in the storage modulus with increasing the strain amplitude. The lowest storage modulus is exhibited by the full-NP-network polymer composites system at a low strain amplitude, indicating that a perfect NP-network structure contributes significantly to the reduction of NPs-NPs interactions and the increase of the polymer-nanoparticle interactions. The matrix polymer chains can intrude into the NP-network structure, which considerably decreases the NPs-NPs interactions. The breakdown of the NPs-NPs interactions can be negligible when increasing the strain within low strain amplitude range, compared to the non-NP-network structure, suggesting that the NP-network structure enhances

the interactions between the matrix polymer chains and NPs as well as dramatically decreases the Payne effect at small strain amplitude.

Interestingly, a slight increase of the storage modulus at the strain amplitude ranging approximately from 5% to 9% is observed, which can be explained by the competition between the NPs-NPs interactions and the NPs-polymers interactions. The breakdown of the NPs-NPs interactions decreases the storage modulus, while the intruding matrix polymer chains will interact with the NP network, resulting in stronger physical crosslinking with increasing elastic response, which consequently leads to a slight increase of the storage modulus. This phenomenon is particularly distinct in the full-NP-network polymer composites system, which exactly reflects stronger interactions between the polymer matrix and the NP network. It is notable that at the large strain amplitude, the storage modulus shows a completely opposite location to that of at the small strain amplitude in the four systems, which is in association with the breakdown of the NPs-NPs interactions. A perfect NP network system will surely maintain a relatively moderate as well as stable NPs-NPs interactions when suffering the cyclic dynamic shear, unlike the non-NP-network system, whose NPs-NPs interactions may risk a devastating destruction under the large shear strain amplitude.

4. Conclusions

An integrated structure of NP network, in which NPs are connected by dual-end functionalized short chains, immersed in the polymeric matrix is successfully fabricated. Firstly, we investigate the effects of the dual-end grafted chain flexibility and density on the dispersion of the NPs and the spatial dimension of the polymer matrix chains. A uniform dispersion of NPs and the most distinct penetration state of

polymer matrix into the NP network is gained when the grafted chain flexibility and density is moderate, such as when $N_g = 250$, $k = 500$ .After that, by purely changing the interaction strength between the matrix polymer chains and the grafted ones while fixing the number of the grafted chains and its flexibility, we note that the interfacial contacts between polymer matrix and the NP network increase obviously with the increase of the interaction strength between the grafted polymer chains and the matrix polymer chains. This was demonstrated by calculating the total interaction energy between the polymer matrix chains and the grafted chains. Furthermore, the uniaxial stress-strain behavior and the orientation extent along the deformation direction of the matrix and grafted polymer chains influenced by the interaction strength between the matrix polymer and the grafted chains are investigated both for the uncross-linked single-network system and the cross-linked double-network system. Consequently, more mechanical reinforcement is obtained when increasing the interaction strength between the matrix polymer and the grafted chains in both systems. The grafted chains orient more strikingly than that of the polymer matrix chains, which results from the pulling effect of the NPs. Particularly, for the double-network system, we regulate the integrity of the NP network ranging from 0% to 100%, corresponding to the transition of the dispersion morphology of the NPs from the aggregation state to the homogeneous dispersion state, to examine its effect on the mechanical behavior. The mechanical reinforcing efficiency, indicated by the tensile stress strength variation, increases accompanying with the increase of the integrity of the NP network, attributed to the much greater orientation of grafted and matrix polymer chains induced by the enhanced dispersion of the NPs. Moreover, by simulating the storage modulus as a function of the strain amplitude in the single-network system, the non-linear behavior (Payne effect) is seen to decrease with the increase of the NP

network integrity due to the improved dispersion of the NPs. In conclusion, the structure of the NP network embedded in the polymer matrix obtained in our study has proved to be effective in realizing the uniform dispersion of NPs and tailoring the mechanical properties of the polymer matrix, hopefully providing a new approach to design and fabricate high performance polymer nanocomposites.

References

1. Tang, Z. H.; Huang, J.; Guo, B. C.; Zhang, L. Q.; Liu, F. Bioinspired Engineering of Sacrificial Metal-Ligand Bonds into Elastomers with Supramechanical Performance and Adaptive Recovery. *Macromolecules* **2016,***49* (5), 1781-1789.
2. Gold, B. J.; Hovelmann, C. H.; Weiss, C.; Radulescu, A.; Allgaier, J.; Pyckhout-Hintzen, W.; Wischnewski, A.; Richter, D. Sacrificial bonds enhance toughness of dual polybutadiene networks. *Polymer* **2016,***87*, 123-128.
3. Creton, C. Toughening elastomers with sacrificial bonds and watching them break. *Science* **2014,***344* (6180), 186-189.
4. Zhang, X. H.; Tang, Z. H.; Huang, J.; Lin, T. F.; Guo, B. C. Strikingly Improved Toughness of Nonpolar Rubber by Incorporating Sacrificial Network at Small Fraction. *J. Polym. Sci. Pt. B-Polym. Phys.* **2016,***54* (8), 781-786.
5. Li, H. Y.; Yang, L.; Weng, G. S.; Xing, W.; Wu, J. R.; Huang, G. S. Toughening rubbers with a hybrid filler network of graphene and carbon nanotubes. *J. Mater. Chem. A* **2015,***3* (44), 22385-22392.
6. Liu, J.; Lu, Y. L.; Tian, M.; Li, F.; Shen, J. X.; Gao, Y. Y.; Zhang, L. Q. The Interesting Influence of Nanosprings on the Viscoelasticity of Elastomeric Polymer Materials: Simulation and Experiment. *Advanced Functional Materials* **2013,***23* (9), 1156-1163.
7. Urk, D.; Demir, E.; Bulut, O.; Cakiroglu, D.; Cebeci, F. C.; Ovecoglu, M. L.; Cebeci, H. Understanding the polymer type and CNT orientation effect on the dynamic mechanical properties of high volume fraction CNT polymer nanocomposites. *Compos. Struct.* **2016,***155*, 255-262.
8. Wang, L.; Zheng, Z. J.; Davris, T.; Li, F. Z.; Liu, J.; Wu, Y. P.; Zhang, L. Q.; Lyulin, A. V. Influence of Morphology on the Mechanical Properties of Polymer Nanocomposites Filled with Uniform or Patchy Nanoparticles. *Langmuir* **2016,***32* (33), 8473-8483.
9. Sen, S.; Thomin, J. D.; Kumar, S. K.; Keblinski, P. Molecular underpinnings of the mechanical reinforcement in polymer nanocomposites. *Macromolecules* **2007,***40* (11), 4059-4067.
10. Jancar, J.; Douglas, J. F.; Starr, F. W.; Kumar, S. K.; Cassagnau, P.; Lesser, A. J.; Sternstein, S. S.; Buehler, M. J. Current issues in research on structure-property relationships in polymer nanocomposites. *Polymer* **2010,***51* (15), 3321-3343.
11. Balazs, A. C.; Emrick, T.; Russell, T. P. Nanoparticle polymer composites: Where two small worlds meet. *Science* **2006,***314* (5802), 1107-1110.

12. Tjong, S. C. Structural and mechanical properties of polymer nanocomposites. *Mater. Sci. Eng. R-Rep.* **2006,***53* (3-4), 73-197.
13. Moll, J. F.; Akcora, P.; Rungta, A.; Gong, S. S.; Colby, R. H.; Benicewicz, B. C.; Kumar, S. K. Mechanical Reinforcement in Polymer Melts Filled with Polymer Grafted Nanoparticles. *Macromolecules* **2011,***44* (18), 7473-7477.
14. Kalb, J.; Dukes, D.; Kumar, S. K.; Hoy, R. S.; Grest, G. S. End grafted polymer nanoparticles in a polymeric matrix: Effect of coverage and curvature. *Soft Matter* **2011,***7* (4), 1418-1425.
15. Kumar, S. K.; Jouault, N.; Benicewicz, B.; Neely, T. Nanocomposites with Polymer Grafted Nanoparticles. *Macromolecules* **2013,***46* (9), 3199-3214.
16. Ginzburg, V. V. Polymer-Grafted Nanoparticles in Polymer Melts: Modeling Using the Combined SCFT-DFT Approach. *Macromolecules* **2013,***46* (24), 9798-9805.
17. Moll, J.; Kumar, S. K.; Snijkers, F.; Vlassopoulos, D.; Rungta, A.; Benicewicz, B. C.; Gomez, E.; Ilavsky, J.; Colby, R. H. Dispersing Grafted Nanoparticle Assemblies into Polymer Melts through Flow Fields. *Acs Macro Letters* **2013,***2* (12), 1051-1055.
18. Ruan, Y. B.; Gao, L.; Yao, D. D.; Zhang, K.; Zhang, B. Q.; Chen, Y. M.; Liu, C. Y. Polymer-Grafted Nanoparticles with Precisely Controlled Structures. *Acs Macro Letters* **2015,***4* (10), 1067-1071.
19. Akcora, P.; Liu, H.; Kumar, S. K.; Moll, J.; Li, Y.; Benicewicz, B. C.; Schadler, L. S.; Acehan, D.; Panagiotopoulos, A. Z.; Pryamitsyn, V.; Ganesan, V.; Ilavsky, J.; Thiyagarajan, P.; Colby, R. H.; Douglas, J. F. Anisotropic self-assembly of spherical polymer-grafted nanoparticles. *Nat. Mater.* **2009,***8* (4), 354-U121.
20. Chao, H. K.; Riggleman, R. A. Effect of particle size and grafting density on the mechanical properties of polymer nanocomposites. *Polymer* **2013,***54* (19), 5222-5229.
21. Yan, L. T.; Xie, X. M. Computational modeling and simulation of nanoparticle self-assembly in polymeric systems: Structures, properties and external field effects. *Progress in Polymer Science* **2013,***38* (2), 369-405.
22. Liu, J.; Zheng, Z. J.; Li, F. Z.; Lei, W. W.; Gao, Y. Y.; Wu, Y. P.; Zhang, L. Q.; Wang, Z. L. Nanoparticle chemically end-linking elastomer network with super-low hysteresis loss for fuel-saving automobile. *Nano Energy* **2016,***28*, 87-96.
23. Wang, Z. X.; Zheng, Z. J.; Liu, J.; Wu, Y. P.; Zhang, L. Q. Tuning the Mechanical Properties of Polymer Nanocomposites Filled with Grafted Nanoparticles by Varying the Grafted Chain Length and Flexibility. *Polymers* **2016,***8* (9), 20.
24. Zheng, Z. J.; Wang, Z. X.; Wang, L.; Liu, J.; Wu, Y. P.; Zhang, L. Q. Dispersion and shear-induced orientation of anisotropic nanoparticle filled polymer nanocomposites: insights from molecular dynamics simulation. *Nanotechnology* **2016,***27* (26), 15.
25. Zheng, Z. J.; Li, F. Z.; Liu, H. J.; Shen, J. X.; Liu, J.; Wu, Y. P.; Zhang, L. Q.; Wang, W. C. Tuning the structure and mechanical property of polymer nanocomposites by employing anisotropic nanoparticles as netpoints. *Physical Chemistry Chemical Physics* **2016,***18* (36), 25090-25099.
26. Ducrot, E.; Creton, C. Characterizing Large Strain Elasticity of Brittle Elastomeric Networks by Embedding Them in a Soft Extensible Matrix. *Advanced Functional Materials* **2016,***26* (15), 2482-2492.

27. Baeza, G. P.; Dessi, C.; Costanzo, S.; Zhao, D.; Gong, S. S.; Alegria, A.; Colby, R. H.; Rubinstein, M.; Vlassopoulos, D.; Kumar, S. K. Network dynamics in nanofilled polymers. *Nat. Commun.* **2016,***7*, 6.
28. Seo, G.; Kaang, S.; Hong, C. K.; Jung, D. S.; Ryu, C. S.; Lee, D. H. Preparation of novel fillers, named networked silicas, and their effects of reinforcement on rubber compounds. *Polymer International* **2008,***57* (10), 1101-1109.
29. Seo, G.; Park, S. M.; Ha, K.; Choi, K. T.; Hong, C. K.; Kaang, S. Effectively reinforcing roles of the networked silica prepared using 3,3'-bis(triethoxysilylpropyl)tetrasulfide in the physical properties of SBR compounds. *Journal of Materials Science* **2010,***45* (7), 1897-1903.
30. Li, Y.; Kroger, M.; Liu, W. K. Dynamic structure of unentangled polymer chains in the vicinity of non-attractive nanoparticles. *Soft Matter* **2014,***10* (11), 1723-1737.
31. Kroger, M.; Peleg, O.; Halperin, A. From Dendrimers to Dendronized Polymers and Forests: Scaling Theory and its Limitations. *Macromolecules* **2010,***43* (14), 6213-6224.
32. Shen, J. X.; Liu, J.; Li, H. D.; Gao, Y. Y.; Li, X. L.; Wu, Y. P.; Zhang, L. Q. Molecular dynamics simulations of the structural, mechanical and visco-elastic properties of polymer nanocomposites filled with grafted nanoparticles. *Physical Chemistry Chemical Physics* **2015,***17* (11), 7196-7207.
33. Morris, D.; Morriss, G. Statistical Mechanics of Non-Equilibrium Liquids. Academic Press, London, 1990.
34. Lees, A.; Edwards, S. The computer study of transport processes under extreme conditions. *Journal of Physics C: Solid State Physics* **1972,***5* (15), 1921.
35. Plimpton, S. Fast Parallel Algorithms for Short-Range Molecular Dynamics. *Journal of Computational Physics* **1995,***117* (1), 1-19.
36. Shen, J. X.; Liu, J.; Gao, Y. Y.; Li, X. L.; Zhang, L. Q. Elucidating and tuning the strain-induced non-linear behavior of polymer nanocomposites: a detailed molecular dynamics simulation study. *Soft Matter* **2014,***10* (28), 5099-5113.
37. Liu, J.; Wu, S.; Zhang, L.; Wang, W.; Cao, D. Molecular dynamics simulation for insight into microscopic mechanism of polymer reinforcement. *Physical Chemistry Chemical Physics Pccp* **2011,***13* (2), 518-29.
38. Liu, J.; Shen, J. X.; Gao, Y. Y.; Zhou, H. H.; Wu, Y. P.; Zhang, L. Q. Detailed simulation of the role of functionalized polymer chains on the structural, dynamic and mechanical properties of polymer nanocomposites. *Soft Matter* **2014,***10* (44), 8971-8984.

Table 1.Type, diameter and mass of simulated particles

Atom type	Description	Bead diameter/σ	Bead mass/m
1	Nanoparticles	4	64
2	Functionalized end of grafted chains	1	1
3	Grafted chains	1	1
4	Matrix chains	1	1

Table 2.Potential parameters (ε, σ , cutoff) of the Lennard-Jones potential and bonded potential for different types of simulated particles

Polymer-polymer		NPs-NPs	Polymer-NPs		
			Grafted polymer-NPs		Matrix polymer-NPs
LJ potential	Bonded potential	LJ potential	LJ potential		LJ potential
ε=1.0	k=1000ε/σ^2	ε=1.0	ε=1.0	ε=1.0	ε=1.0
σ=1.0	R_0=1.0σ	σ=1.0	σ=1.0	σ=1.0	σ=1.0
r_{cutoff}=2.5σ		r_{cutoff}=2.5σ	r_{cutoff}=2.5σ (end polymer beads)	r_{cutoff}=1.12σ (other polymer beads)	r_{cutoff}=1.12σ

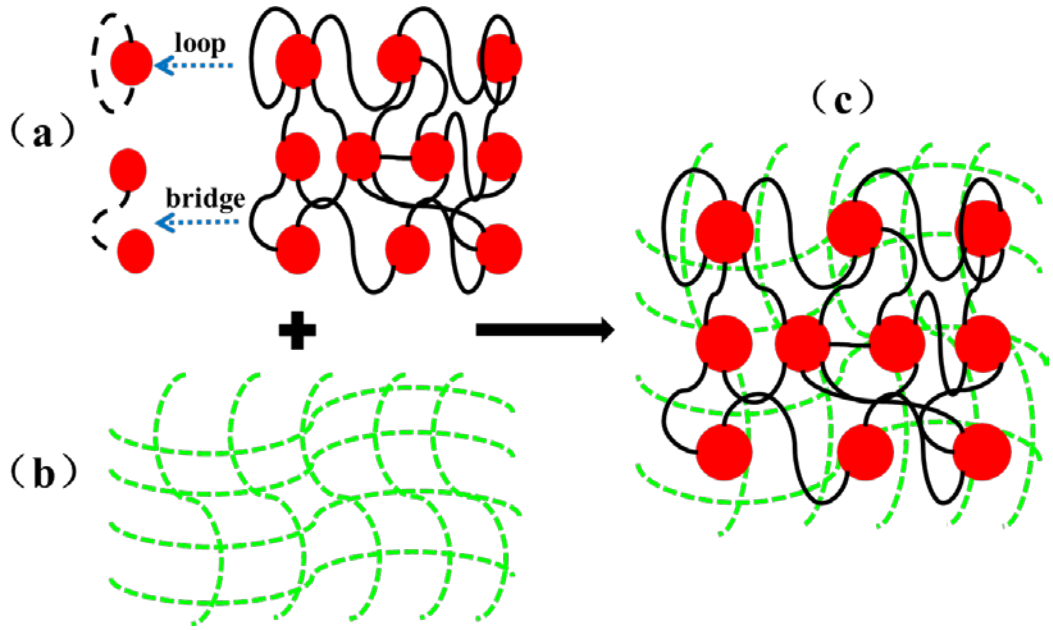

Figure 1.The construction model of the single-network system.(a) The NPs (red spheres) are connected by dual-end functionalized short chains(black segments) to form a NP network(the only network), while (b) the linear matrix polymeric chains (green segments) are not crosslinked (no network) initially.

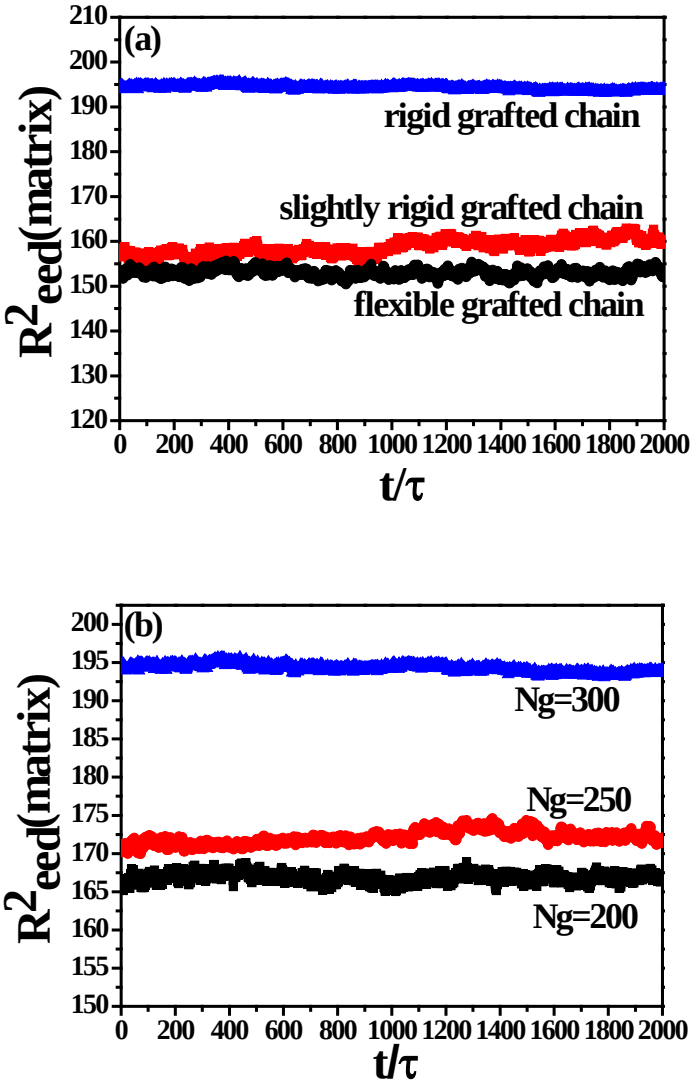

Figure 2.(a)The mean-squared end-to-end distance $R^2_{eed}$of the matrix polymeric chains with varying grafted chains flexibility (larger bending energies represent more rigid grafted chains. Here $k = 0$, $k = 500$ and $k = 1000$ denote flexible, slightly rigid and strong rigid grafted chains, respectively); (b) the mean-squared end-to-end distance R^2_{eed} of the matrix polymeric chains with varying grafted chains number (N_g)as a function of the simulation time in the single-network systems.

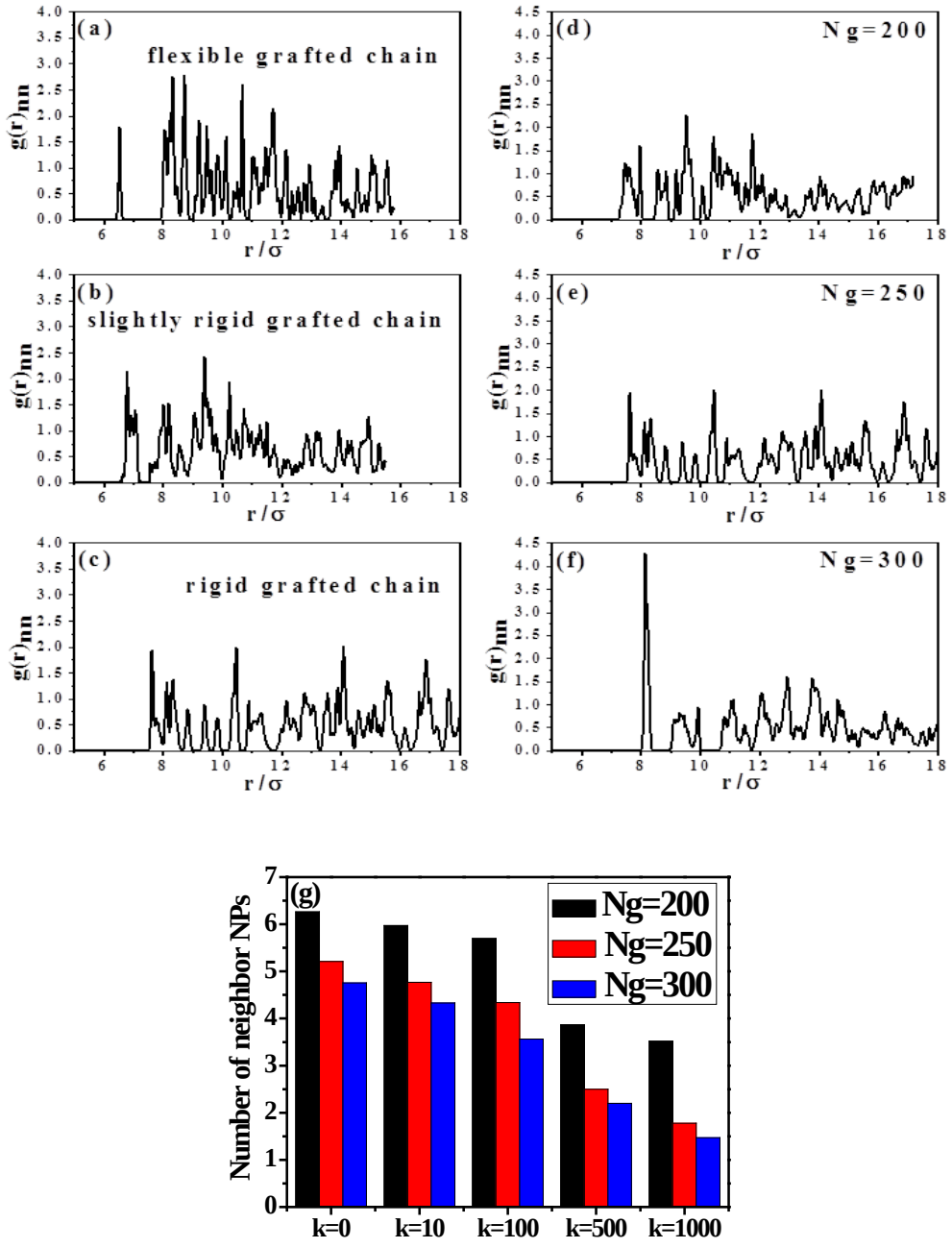

Figure 3. (a)(b)(c) and (d)(e)(f) demonstrate the radial distribution functions of NPs-NPs as a function of the effect of the grafted chain flexibility(Here $k=0$, $k=500$ and $k=1000$ denote flexible, slightly rigid and strong rigid grafted chains, respectively) and the effect of the number of the grafted chains (N_g), respectively in single-network systems; (g) the number of NPs within a distance

of r<12.0 from each NP, by varying the grafting chain density and chain flexibility (the increase of the value of k denotes more rigidity of chains).

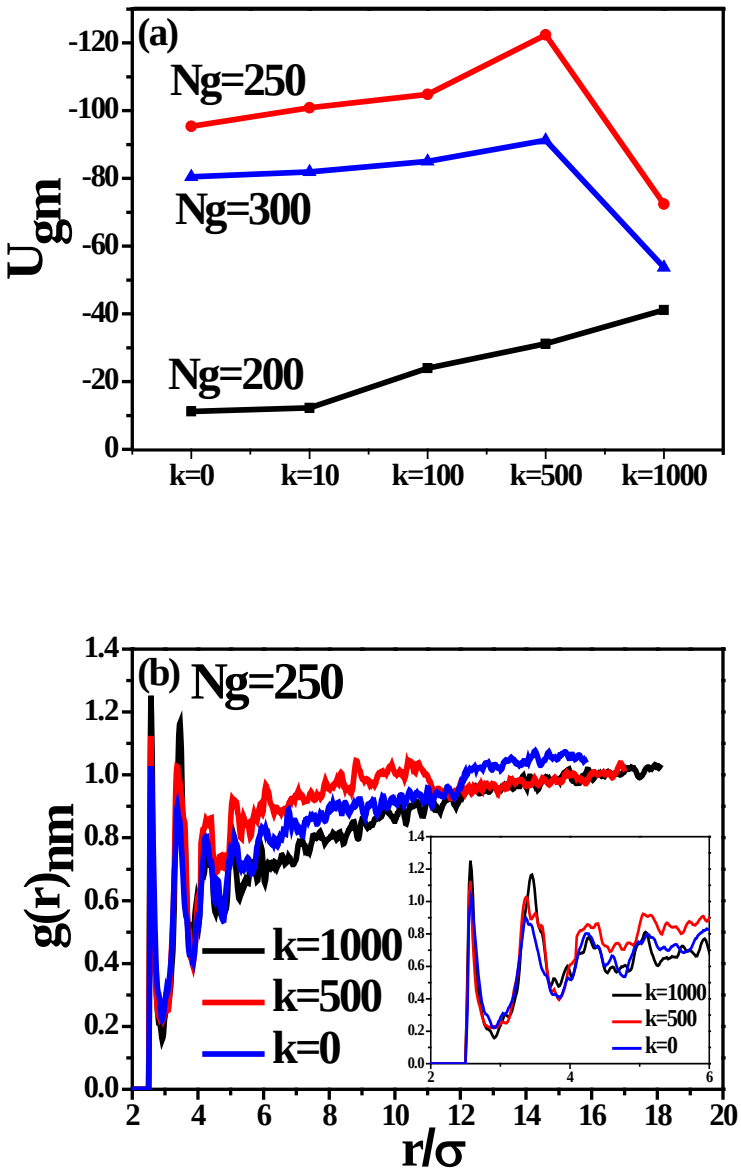

Figure 4. (a)The total interaction energy U_{gm} between matrix polymer chains and short grafted chains as a function of the grafted chain flexibility as well as the number of the grafted chains. The increase of the value of k denotes the increase of the grafted chain rigidity; (b) the radial distribution function between

NPs and the matrix polymer chains beads by adjusting the flexibility of the grafted chains at $N_g = 250$ in single-network systems.

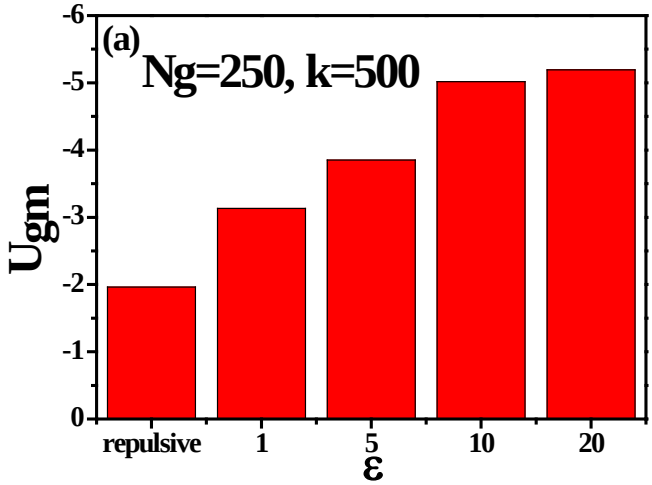

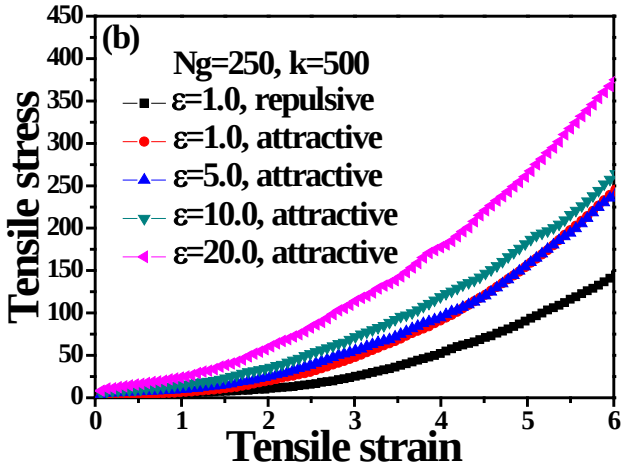

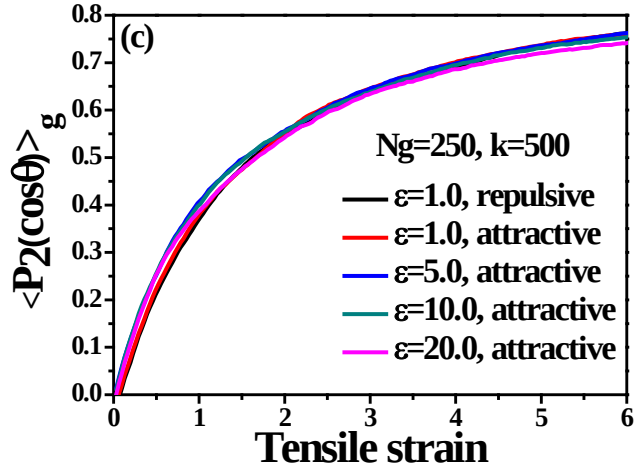
(c)
Ng=250, k=500
ε=1.0, repulsive
ε=1.0, attractive
ε=5.0, attractive
ε=10.0, attractive
ε=20.0, attractive
<P2(cosθ)>g
Tensile strain

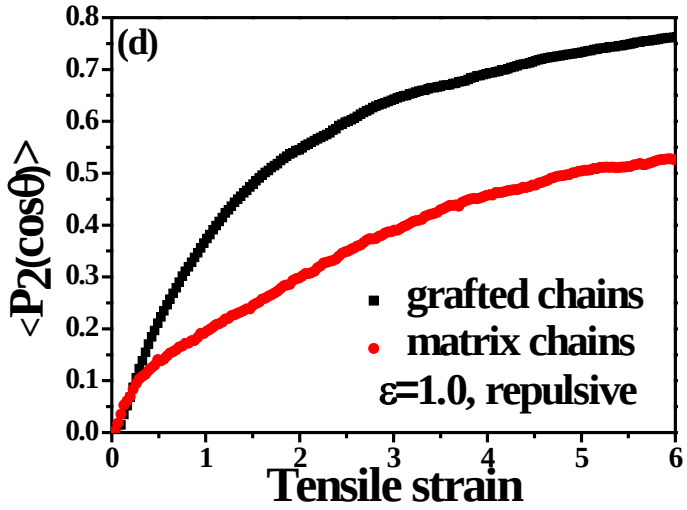
(d)
grafted chains
matrix chains
ε=1.0, repulsive
<P2(cosθ)>
Tensile strain

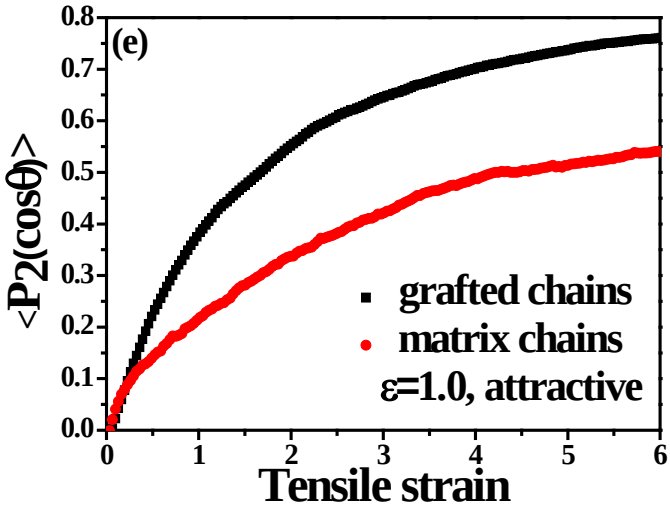
(e)
grafted chains
matrix chains
ε=1.0, attractive
<P2(cosθ)>
Tensile strain

Figure 5. The effect of the interfacial interaction strength between matrix polymers and grafted chains on (a) the interfacial structure by calculating the total interaction energy U_{gm} between the matrix polymer chains and the grafted chains, (b) the tensile stress-strain behavior, (c) the orientation of the grafted chains of the single-network system. (d), (e) Comparison of the orientation of the grafted chains with that of the matrix polymer chains with different interfacial interactions during tensile process for the single-network system.

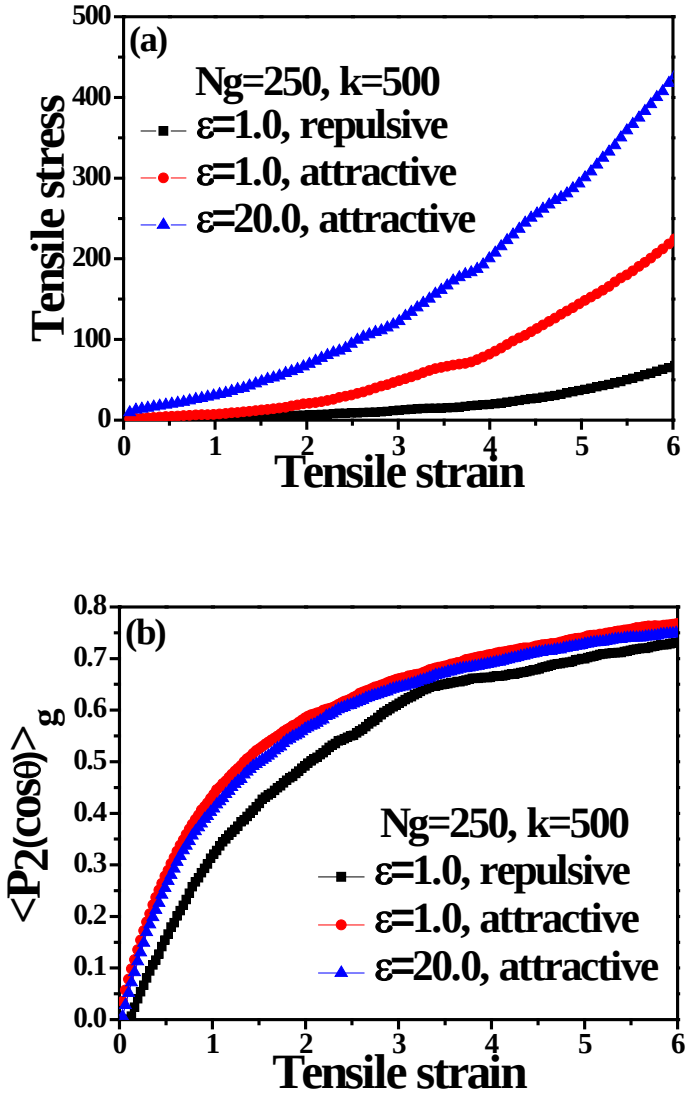

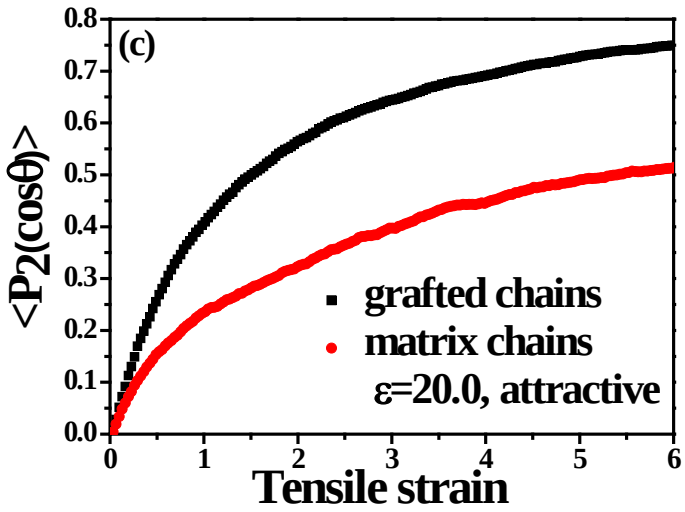

Figure 6. The effect of the interfacial interaction strength between matrix polymers and grafted chains on (a) the tensile stress-strain behavior, (b) the orientation of the grafted chains during the tensile process for the double-network system. (c)Comparison of the orientation of the grafted chains with that of the matrix polymer chains when the interfacial interaction parameter is set as ε=20.0 for the double-network system.

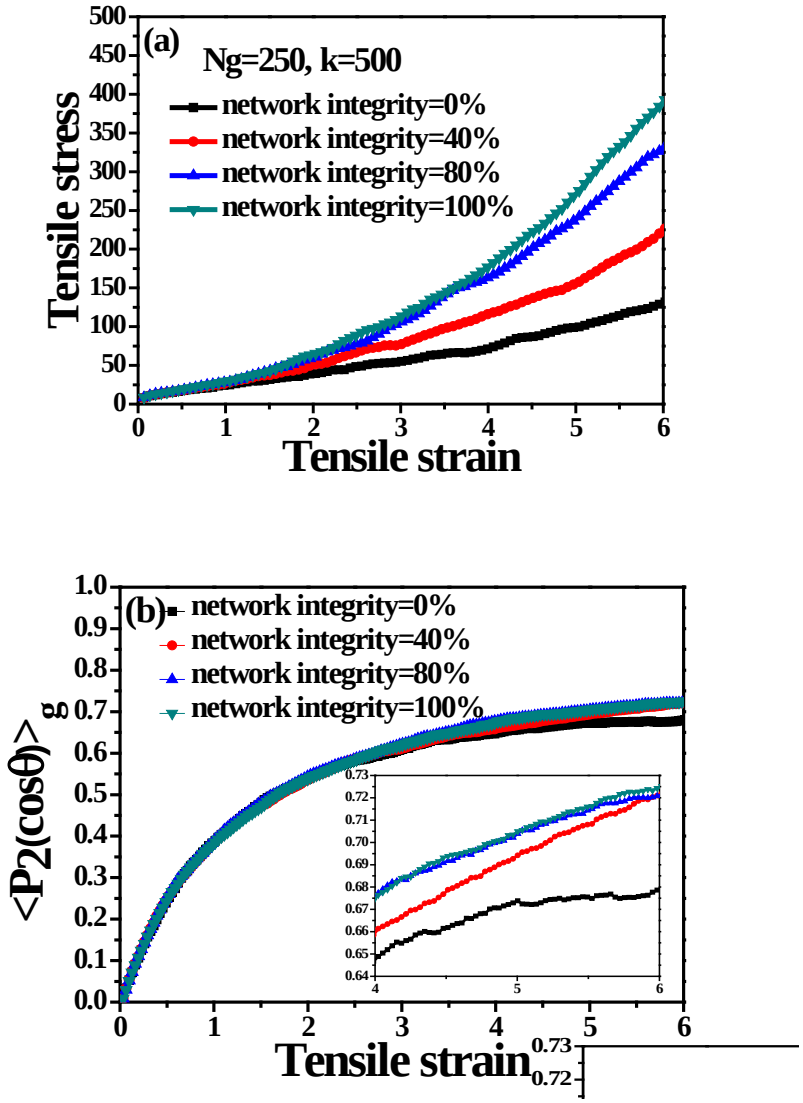

Figure 7. The effect of the NP network integrity(the ratio of the number of the crosslinked bonds of the partial NP network to that of a perfect NP network)on (a)the tensile stress-strain behavior , (b)the grafted chains orientation during the tensile process of the double-network system.

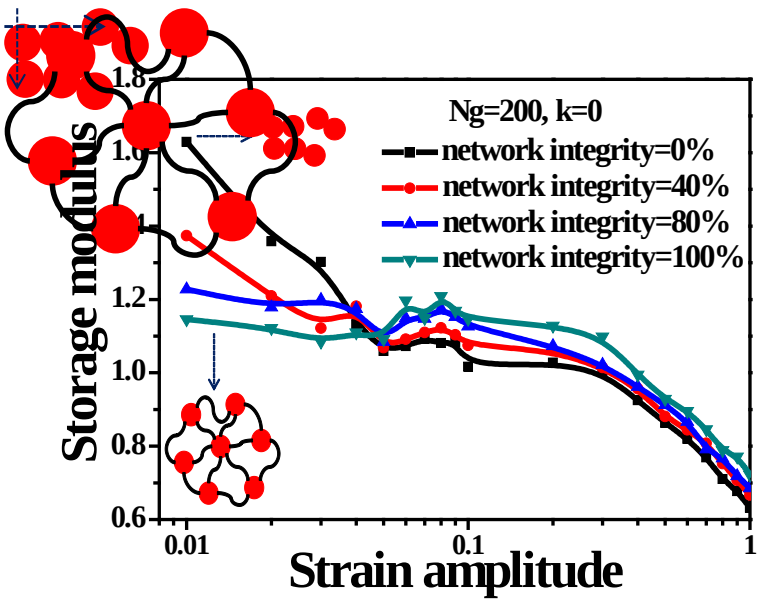

Figure 8. The storage modulus as a function of the dynamic cyclic shear strain amplitude for the single-network systems with varying degree of integrity of NPs network(the ratio of the number of the crosslinked bonds of the partial NP network to that of a perfect NP network).A larger NP network integrity signifies a less-broken NP network.